

Modeling the fission yeast cell cycle: Quantized cycle times in *wee1⁻cdc25 Δ* mutant cells

Akos Sveiczzer*[†], Attila Csikasz-Nagy*, Bela Gyorffy*, John J. Tyson[‡], and Bela Novak*

*Department of Agricultural Chemical Technology, Budapest University of Technology and Economics, 1521 Budapest, Szt. Gellert ter 4, Hungary; and [‡]Department of Biology, Virginia Polytechnic Institute and State University, Blacksburg, VA 24061

Edited by Paul Nurse, Imperial Cancer Research Fund, London, United Kingdom, and approved April 17, 2000 (received for review January 4, 2000)

A detailed mathematical model for the fission yeast mitotic cycle is developed based on positive and negative feedback loops by which Cdc13/Cdc2 kinase activates and inactivates itself. Positive feedbacks are created by Cdc13/Cdc2-dependent phosphorylation of specific substrates: inactivating its negative regulators (Rum1, Ste9 and Wee1/Mik1) and activating its positive regulator (Cdc25). A slow negative feedback loop is turned on during mitosis by activation of Slp1/anaphase-promoting complex (APC), which indirectly re-activates the negative regulators, leading to a drop in Cdc13/Cdc2 activity and exit from mitosis. The model explains how fission yeast cells can exit mitosis in the absence of Ste9 (Cdc13 degradation) and Rum1 (an inhibitor of Cdc13/Cdc2). We also show that, if the positive feedback loops accelerating the G₂/M transition (through Wee1 and Cdc25) are weak, then cells can reset back to G₂ from early stages of mitosis by premature activation of the negative feedback loop. This resetting can happen more than once, resulting in a quantized distribution of cycle times, as observed experimentally in *wee1⁻cdc25 Δ* mutant cells. Our quantitative description of these quantized cycles demonstrates the utility of mathematical modeling, because these cycles cannot be understood by intuitive arguments alone.

An important feature of the eukaryotic cell cycle is the strict alternation of DNA synthesis (S phase) and mitosis (M phase), enforced by enzymes, called cyclin-dependent kinases (CDKs), that regulate the activities of many proteins involved in the mechanics of genome replication and nuclear division (1). CDKs are active only in partnership with regulatory subunits, called cyclins. In lower eukaryotes like yeasts, there is only one essential CDK subunit (Cdk1), called Cdc2 in fission yeast. Cdc2 combines with three different B-type cyclins (Cig1, Cig2, and Cdc13), but only Cdc13 is essential to drive a complete cell cycle (2). Proper execution of the cell cycle requires that Cdc13/Cdc2 activity oscillates between low (G₁), intermediate (S and G₂), and high (M) levels (3). These different cell cycle phases are achieved by antagonistic relationships between Cdc13/Cdc2 kinase and its negative regulators (Ste9, Rum1, and Wee1/Mik1) (4). In G₁ phase, Cdc13 level is low because Ste9 (also known as Srw1) targets Cdc13 for ubiquitination by the anaphase-promoting complex (APC, also known as cyclosome) and ultimately for degradation by proteasomes. In addition, G₁ cells contain abundant Rum1, a stoichiometric inhibitor of the Cdc13/Cdc2 complex (5). At the G₁/S transition, both Ste9 (M. Blanco, A. Sanchez-Diaz, and S. Moreno, personal communication) and Rum1 (6) are phosphorylated, which inactivates Ste9 and promotes degradation of Rum1. As a consequence, the Cdc13 level starts to rise and cells enter S phase. However, Cdc13/Cdc2 kinase activity is depressed by phosphorylation of the Tyr-15 residue of Cdc2 by two tyrosine kinases, Wee1 and Mik1, during S and G₂ phases. Mik1 is kept active by unrepliated DNA (7), whereas Wee1 is active during early G₂. In late G₂, Wee1 is phosphorylated and inactivated by Cdc13/Cdc2 (8). The inhibitory phosphate group on Tyr-15 of Cdc2 is removed by a phosphatase, Cdc25, which is activated by Cdc13/Cdc2 at this time (9).

At the end of the cycle, all of the negative regulators are turned back on, Cdc13/Cdc2 kinase activity is lost, and the cell leaves mitosis. The mechanism of activation of the negative regulators is largely unknown in fission yeast. In budding yeast, a phosphatase (Cdc14) has been shown to up-regulate the corresponding negative regulators, Sic1 and Cdh1 (10, 11). Here we propose a similar mechanism working in fission yeast, in which a yet unknown phosphatase, analogous to Cdc14, dephosphorylates Rum1, Ste9, and the tyrosine-modifying enzymes (Wee1, Mik1, and Cdc25). With this model in hand, we show how fission yeast cells exit mitosis in the absence of Ste9 and Rum1. As a bonus, we observe an interesting resetting mechanism from early stages of mitosis back to G₂ phase, which explains the curious quantized cycles of fission yeast mutant cells (*wee1⁻cdc25 Δ*) lacking the major G₂/M regulators (12).

The Model

Our present model (Fig. 1) is a combination of several earlier efforts (4, 13, 14). At its core are antagonistic interactions between Cdc13/Cdc2 (M-phase promoting factor, MPF) and its negative regulators, Ste9, Rum1, and Wee1/Mik1. Ste9 targets Cdc13 subunits for ubiquitination by the APC (15, 16). Rum1 is a cyclin-dependent kinase inhibitor, which reversibly binds to Cdc13/Cdc2 and inhibits its activity (17). Wee1 and Mik1 are tyrosine kinases that phosphorylate the Cdc2 subunit on Tyr-15, thereby inhibiting its activity (18, 19). MPF phosphorylates all its negative regulators, and this phosphorylation is either inhibitory, as in the case of Ste9 (M. Blanco *et al.*, personal communication) and Wee1 (8), or promotes degradation of the molecule (Rum1) (6). By inactivating the proteins that oppose it, Cdc13/Cdc2 promotes its own activation (“positive feedback”).

In addition to inhibiting its enemies, MPF also activates its friend, Cdc25, the tyrosine phosphatase that converts preMPF (the tyrosine phosphorylated form of Cdc13/Cdc2) into active MPF (20). In the absence of Cdc25, a backup phosphatase, Pyp3, can do the job less effectively (21).

Cdc13/Cdc2 is helped to phosphorylate its enemies by Cdc2 subunits complexed to other cyclins (Puc1, Cig1, and Cig2) (22) that are less sensitive to Rum1 inhibition (23) and/or Ste9/APC-dependent degradation (M. Blanco *et al.*, personal communication). For simplicity, these cyclin/Cdc2 complexes are lumped together in the model as a starter kinase (SK or Cdc2/X), with constant activity. The transition from mitosis to G₁ is achieved by a negative feedback loop in which Cdc13/Cdc2 indirectly up-regulates its negative regulators by turning on a protein phosphatase (PP) analogous to Cdc14 in budding yeast (14). In our model, MPF activates Slp1/APC (24), which degrades a hypothetical inhibitor of PP. We propose that in fission yeast PP dephosphorylates the tyrosine-modifying enzymes

This paper was submitted directly (Track II) to the PNAS office.

Abbreviations: CDK, cyclin-dependent protein kinase; MPF, M-phase promoting factor; APC, anaphase-promoting complex; PP, protein phosphatase; WT, wild type; preMPF, Tyr-15-phosphorylated MPF; CT, cycle time; BL, birth length; SK, starter kinase.

[†]To whom reprint requests should be addressed. E-mail: sveiczzer.mkt@chem.bme.hu.

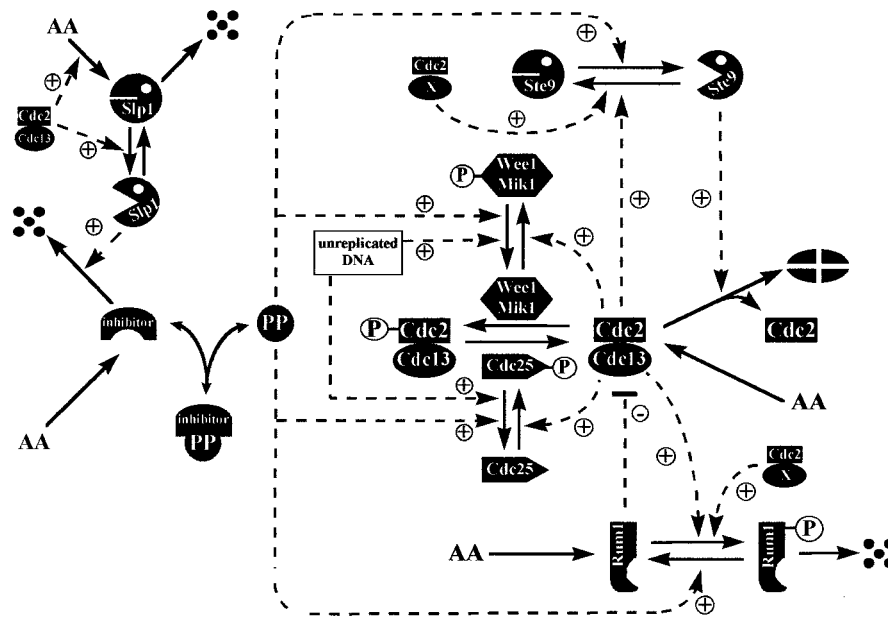


Fig. 1. A molecular mechanism for the regulation of Cdc13-associated kinase activity in fission yeast. All of the events of the fission yeast cell cycle can be orchestrated by fluctuations of the activity of a single cyclin-dependent kinase, Cdc13/Cdc2. Cdc13 is synthesized from amino acids (AA) and combines readily with catalytic subunits, Cdc2, which are assumed to be always present in excess. The activity of Cdc13/Cdc2 is modulated by Rum1 inhibition, by Tyr-15 phosphorylation (via Wee1 and Mik1, which is reversed by Cdc25 and Pyp3; the last molecule is not shown on figure), and by Ste9-dependent cyclin degradation. Other cyclins (Puc1, Cig1, and Cig2, which are represented by X on the figure) in complex with Cdc2 can assist these processes.

(Wee1, Mik1, and Cdc25), as well as Rum1 and Ste9, thereby down-regulating the activity of Cdc13/Cdc2.

The mechanism in Fig. 1 is converted into a set of differential equations by using standard principles of biochemical kinetics (Table 1). After specifying the numerical values of numerous rate constants and Michaelis constants in these equations, numerical solution gives the concentrations of the variables as functions of time. Numerical values of the parameters were chosen so that the concentration profiles of cell cycle regulators are consistent with experiments on wild-type (WT) and mutant cells.

Simulations with the Deterministic Model

The simulated cell cycle of WT fission yeast is presented in Fig. 2. The cell is born at a relative mass of 1, grows exponentially in time, and at a mass of 2 divides symmetrically into two identical daughter cells. During the short G₁ phase (Fig. 2, Table 2), Cdc13/Cdc2 activity is kept low by high activities of Ste9, Rum1, and Wee1. (Nonetheless, our simplified version of G₁/S control in this model overestimates the duration of G₁ phase.) Soon after mitosis, Cdc13 level starts to rise as SK switch off Ste9 and promote degradation of Rum1. However, Cdc13/Cdc2 cannot be fully activated because Wee1 and Mik1 remain active. We assume that the tyrosine-phosphorylated form of Cdc13/Cdc2 retains some activity (5% of the unphosphorylated form), and this activity is sufficient to initiate DNA synthesis (with the help of SK). Meanwhile, cells are growing, and larger cells (we assume) synthesize Cdc13 at a faster rate, so the nuclear concentration of Cdc13/Cdc2 increases. When MPF activity in the nucleus reaches a threshold value, it inactivates Wee1 (and Mik1) and activates Cdc25. As a result, preMPF is converted autocatalytically to active MPF, and the cell enters mitosis. Sister chromatids are rapidly aligned on the mitotic spindle, and then MPF activates Slp1/APC, which releases PP from its inactive complex with inhibitor. PP then activates Wee1, Mik1, Ste9, and Rum1, bringing the cell back into G₁ phase. Observe that, before mitotic exit, there is a considerable peak in the tyrosine-

phosphorylated form of Cdc13/Cdc2 (Fig. 2) because Wee1 and Mik1 get activated slightly earlier than Ste9/APC.

With the parameter set in Table 1, we could easily simulate different cell cycle mutants (temperature-sensitive and loss-of-function) by reducing or zeroing the appropriate parameter values. Table 2 summarizes some properties of these simulations. Because many of these mutants have been described by our earlier model (4), they are not discussed further here.

Because tyrosine phosphorylation plays a role in inactivation of Cdc13/Cdc2 at the end of mitosis, *wee1*⁻ mutants spend more time in the high Cdc13/Cdc2 activity state (mitosis), compared with WT cells (see all of the mutants with *wee1*⁻ background in Table 2). This is consistent with experiments showing that *wee1*⁻ mutants spend more time between mitosis and cytokinesis (26). Our model also correctly describes the phenotypes of *mik1Δ*, *cdc25*⁻, and *pyp3Δ* single and *mik1Δ wee1*^{ts} double mutants (Table 2).

The *rum1Δ* mutant of fission yeast grows normally; however, a *rum1Δ wee1*^{ts} double mutant, after a shift-up to the restrictive temperature, becomes progressively smaller and dies (Table 2) (27). Deletion of *ste9* has a similar effect: viable in *wee1*⁺ and lethal in *wee1*⁻ backgrounds (15, 16). In our simulations, Rum1 cannot accumulate during the short G₁ phase in *ste9Δ* mutants, and consequently *ste9Δ wee1*^{ts} double mutant cells die similarly to the *rum1Δ wee1*^{ts} mutant.

Recent observations show that fission yeast survives in the absence of both Rum1 and Ste9 (16), in contrast to the lethality of the homologous budding yeast mutant (*cdh1*⁻ *sic1*⁻) (28). This difference in viability can be attributed to a species-specific difference either in cyclin degradation (Slp1 may be more effective in degrading Cdc13 in fission yeast than is Cdc20 in degrading mitotic cyclins in budding yeast), or in inhibitory tyrosine phosphorylation of Cdk1 (fission yeast activates tyrosine kinases during its normal mitotic cycle, whereas budding yeast does not). We prefer the latter hypothesis, and our simulations of *ste9Δ rum1Δ* (Fig. 3) show that these cells could

Table 1. A mathematical model of the proposed mechanism (Fig. 1) for the fission yeast cell cycle

Differential equations*

$$\frac{d}{dt} Rum1 = k_5 - k'_6 \cdot Rum1 - k_p \cdot (MPF_a + \varepsilon_p \cdot SK \cdot mass) \cdot Rum1 + (k'_{pp} + k_{pp} \cdot PP) \cdot Rum1P - k_j \cdot MPF \cdot Rum1 + k_{JR} \cdot CR + k_{2c} \cdot CR$$

$$\frac{d}{dt} Rum1P = k_p \cdot (MPF_a + \varepsilon_p \cdot SK \cdot mass) \cdot Rum1 - (k'_{pp} + k_{pp} \cdot PP) \cdot Rum1P - (k'_6 + k_6) \cdot Rum1P - k_j \cdot MPF \cdot Rum1P + k_{JR} \cdot CRP + k_{2c} \cdot CRP$$

$$\frac{d}{dt} CR = k_j \cdot MPF \cdot Rum1 - k_{JR} \cdot CR - k_{2c} \cdot CR - k'_6 \cdot CR - k_p \cdot (MPF_a + \varepsilon_p \cdot SK \cdot mass) \cdot CR + (k'_{pp} + k_{pp} \cdot PP) \cdot CRP$$

$$\frac{d}{dt} CRP = k_p \cdot (MPF_a + \varepsilon_p \cdot SK \cdot mass) \cdot CR - (k'_{pp} + k_{pp} \cdot PP) \cdot CRP + k_j \cdot MPF \cdot Rum1P - k_{JR} \cdot CRP - k_{2c} \cdot CRP - (k'_6 + k_6) \cdot CRP$$

$$\frac{d}{dt} MPF = k_1 \cdot mass - k_2 \cdot MPF - k_{Wee} \cdot MPF + k_{C25} \cdot preMPF - k_j \cdot MPF \cdot (Rum1 + Rum1P) + k_{JR} \cdot (CR + CRP) + k'_6 \cdot CR + (k'_6 + k_6) \cdot CRP$$

$$\frac{d}{dt} preMPF = k_{Wee} \cdot MPF - k_{C25} \cdot preMPF - k_2 \cdot preMPF$$

$$\frac{d}{dt} Ste9 = (k'_{Ste9R} + k_{Ste9R} \cdot PP) \cdot \frac{1 - Ste9}{J_{Ste9R} + 1 - Ste9} - k_{Ste9} \cdot (MPF_a + SK \cdot mass) \cdot \frac{Ste9}{J_{Ste9} + Ste9}$$

$$\frac{d}{dt} Mik1 = (k_5 + k'_{MR} + k_{MR} \cdot PP) \cdot \frac{1 - Mik1}{J_{MikR} + 1 - Mik1} - k_M \cdot MPF_a \cdot \frac{Mik1}{J_{Mik} + Mik1}$$

$$\frac{d}{dt} Wee1 = (k'_{WR} + k_{WR} \cdot PP) \cdot \frac{1 - Wee1}{J_{WeeR} + 1 - Wee1} - k_W \cdot MPF_a \cdot \frac{Wee1}{J_{Wee} + Wee1}, \quad \frac{d}{dt} Cdc25 = k_{25} \cdot MPF_a \cdot \frac{1 - Cdc25}{J_{25} + 1 - Cdc25} - (k_5 + k'_{25R} + k_{25R} \cdot PP) \cdot \frac{Cdc25}{J_{25R} + Cdc25}$$

$$\frac{d}{dt} Slp1 = k_{as} \cdot MPF_a - k_{ad} \cdot Slp1, \quad \frac{d}{dt} Slp1_a = (k'_{aa} + k_{aa} \cdot MPF_a) \cdot (Slp1 - Slp1_a) - k_{ai} \cdot Slp1_a - k_{ad} \cdot Slp1_a, \quad \frac{d}{dt} Inh = k_3 - k_i \cdot Inh \cdot PP + k_{iR} \cdot PI - k_4 \cdot Inh$$

$$\frac{d}{dt} PI = k_i \cdot Inh \cdot PP - k_{iR} \cdot PI - k_4 \cdot PI, \quad \frac{d}{dt} mass = \mu \cdot mass, \quad \frac{d}{dt} R_{DNA} = \frac{K}{1 + Y \cdot MPF_a}$$

Rate functions

$$k_2 = V_2 + V_2 \cdot Ste9, k_{2c} = V_{2c} + V_{2c} \cdot Ste9, k_{Wee} = V_{Wee} \cdot Wee1 + V'_{Wee} \cdot (1 - Wee1) + V_{Mik} \cdot Mik1 + V'_{Mik} \cdot (1 - Mik1), k_{C25} = V_{25} \cdot Cdc25 + V'_{25} \cdot (1 - Cdc25) + V_{Pyp} \cdot Pyp3, k_4 = V_4 + V_4 \cdot Slp1_a$$

Auxiliary functions†

$$MPF_a = MPF + \varepsilon \cdot preMPF, PP = 1 - PI$$

Switches

(i) When the ratio MPF_a/PP crosses 0.65 from below, S phase is initiated: R_{DNA} is set to 0, and k_5 is set to $k_{S,max}$. R_{DNA} represents the fraction of DNA which has been replicated; if it reaches 1, then DNA replication is complete, and k_5 is set to $k_{S,min}$. (ii) When MPF_a/PP crosses 0.5 from above, the cell divides functionally ($mass \rightarrow mass/2$), although cytokinesis happens much later in fission yeast. (iii) In normal cases, MPF activity is low during S phase: $Y = 0$, therefore $dR_{DNA}/dt = K = 0.06$, and replication is fast. However, if MPF exceeds 0.2 during replication, then Y is set to 100, therefore the rate of replication decreases. During this delayed S phase, if high MPF activity stimulates mitosis and cell division, the cells consequently die (*cut* phenotype).

Rate constants (for wild-type cells, all have dimensions min^{-1})

$$k_5 = 0.1, k'_6 = 0.1, k_6 = 5, k_p = 100, k'_{pp} = 1, k_{pp} = 100, k_j = 400, k_{JR} = 1, k_1 = 0.02, k_{Ste9} = 5, k'_{Ste9R} = 0.03, k_{Ste9R} = 8, k_M = 1, k'_{MR} = 0.01, k_{MR} = 5, k_W = 2, k'_{WR} = 0.4, k_{WR} = 1, k_{25} = 1, k'_{25R} = 0.4, k_{25R} = 2, k_{as} = 0.1, k_{ad} = 0.1, k'_{aa} = 0.01, k_{aa} = 0.1, k_{ai} = 0.1, k_3 = 0.1, k_i = 50, k_{iR} = 0.5, k_{S,max} = 5, k_{S,min} = 0.1, V_2 = 0.02, V_{2c} = 0.02, V_{2c} = 0.5, V_{Wee} = 10, V'_{Wee} = 0.08, V_{Mik} = 2, V'_{Mik} = 0.04, V_{25} = 10, V'_{25} = 0.05, V_{Pyp} = 0.07, V_4 = 0.01, V_4 = 1, \mu = 0.00462$$

Michaelis and other constants (dimensionless)‡

$$J_{Ste9} = 0.01, J_{Ste9R} = 0.01, J_{Mik} = 0.15, J_{MikR} = 0.15, J_{Wee} = 0.2, J_{WeeR} = 0.2, J_{25} = 0.05, J_{25R} = 0.05, SK = 0.018, \varepsilon = 0.05, \varepsilon_p = 0.025, K = 0.06, Y = 0, Pyp3 = 1$$

*Italicized protein names (e.g., *Cdc25*) refer to the concentration of protein which is a dimensionless number. MPF_a , the total kinase activity of MPF and preMPF; $Rum1P$, concentration of phosphorylated Rum1; CR , concentration of Cdc2/Cdc13/Rum1 trimeric complex; SK , the activity of starter kinases (Cdc2/X); CRP , concentration of Cdc2/Cdc13/Rum1P trimeric complex; $Slp1_a$, the active form of *Slp1*; Inh , concentration of the inhibitor of PP; PI , concentration of PP/Inh dimer complex.

† ε , the kinase activity of preMPF compared to MPF.

‡Because we choose these Michaelis constants all to be considerably smaller than 1, the corresponding enzyme activities, *Ste9*, *Mik1*, *Wee1*, and *Cdc25*, operate as “ultrasensitive” switches (25), i.e., they tend to be either “on” (activity = 1) or “off” (activity = 0).

indeed down-regulate Cdc13/Cdc2 kinase at the end of mitosis by tyrosine phosphorylation. They are indistinguishable from *ste9Δ* simple mutants (Table 2), in which Rum1 does not make a comeback at the end of mitosis. Of course, crossing this strain with *wee1^{ts}* creates a small, nonviable cell at the restrictive temperature (Table 2). Our present model predicts that fission yeast with a single copy of nondegradable *cdc13* [*cdc13dbΔ* mutant (29)] exits mitosis and retains viability (Table 2), similarly to *ste9Δ*, as confirmed by preliminary experiments (J. M. de Prada, M. Blanco and S. Moreno, personal communication).

Fission yeast tolerates even the total absence of Cdc25, if *Wee1* activity is also much reduced (30). At 35°C, the division length of *wee1^{ts} cdc25Δ* double mutant cells is significantly larger, on average, than WT and much more variable (31). Recently, we have shown that quantized cell cycles [with mean cycle times (CT) of 90, 160, and 230 min] underlie this size variability (12), and we proposed that improper regulation of tyrosine phosphorylation could explain this phenomenon (32).

Indeed, our present simulations confirm this proposal: *wee1^{ts} cdc25Δ* cells cannot adjust their CT to the mass doubling time

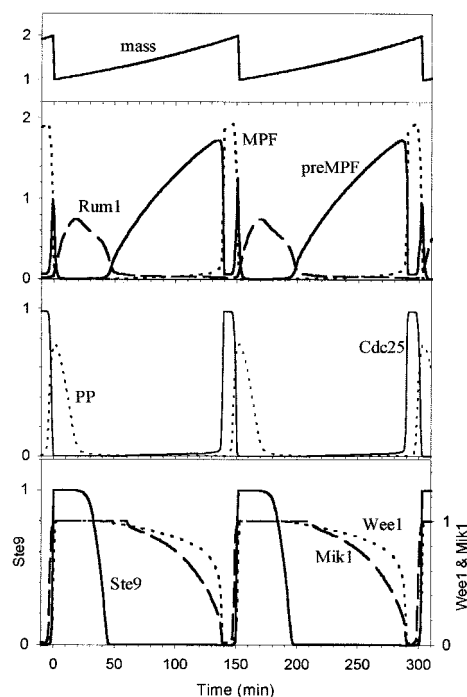


Fig. 2. Numerical simulation of WT cell cycles.

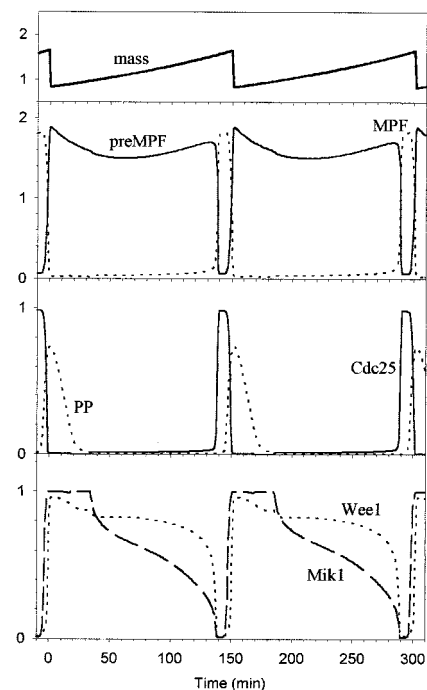


Fig. 3. Numerical simulation of *ste9 rum1Δ* double mutant cells.

($T_d = 150$ min), but instead show shorter (112 min) and longer (170 min) cell cycles in varying occurrence (Fig. 4). Activation of Cdc13/Cdc2 is slow because these mutant cells lack positive feedback in tyrosine modification. However, the negative feedback loop (MPF \rightarrow Slp1/APC \rightarrow PP \rightarrow Mik1, Ste9 and Rum1) is largely intact. In the absence of positive feedback, cell mass has a dramatic effect (through the rate of Cdc13 synthesis) on MPF activation. In small cells, Cdc13 kinase starts to rise, but its activation is slow and Mik1 kinase is turned on prematurely,

before Ste9 and Rum1 can be turned on to reset the cell into G_1 (we propose that Mik1 is a better substrate of PP, than either Ste9 or Rum1). Inhibitory tyrosine phosphorylation (by Mik1 and residual Wee1 activities) causes a drop in Cdc13/Cdc2 kinase activity and resets the cell into G_2 phase rather than to G_1 (the sister chromatids are not separated), from whence it must start new preparations for mitosis. Because the cell did not divide, it is larger in the subsequent G_2 phase; activation of Cdc13/Cdc2 is faster now and MPF turns on Rum1 and Ste9 as

Table 2. Simulated cell-cycle properties of mutant fission yeast strains

Strain	Parameter changes*	Mass at birth (relative)	G_1^+ (min)	S^+ (min)	G_2^+ (min)	M^+ (min)	Comment
WT	—	1.00	38	17	78	17	
<i>wee1^{ts}</i>	$V_{Wee} = 0.08$	0.48	72	18	31	29	
<i>wee1Δ</i>	$V_{Wee} = V_{Wee} = 0$	0.48	73	18	29	30	
<i>mik1Δ</i>	$V_{Mik1} = V_{Mik} = 0$	0.98	39	18	73	20	
<i>mik1Δwee1^{ts}</i>	$V_{Mik1} = V_{Mik} = 0, V_{Wee} = 0.08$	No balanced growth, S and M overlap					<i>cut</i> phenotype
<i>pyp3Δ</i>	$V_{Pyp} = 0$	1.08	36	18	79	17	
<i>cdc25^{ts}</i> or <i>cdc25Δ</i>	$V_{25} = 0.05, V_{25} = 0.00025$ or $V_{25} = V_{25} = 0$	—	—	—	∞	—	G_2 block
<i>wee1^{ts}cdc25Δ[†]</i>	$V_{Wee} = 0.08, V_{25} = V_{25} = 0$	1.22/1.08	22/23	17/17	42/107	31/23	Quantized cycles
<i>wee1^{ts}cdc25Δpyp3Δ</i>	$V_{Wee} = 0.08, V_{25} = V_{25} = 0, V_{Pyp} = 0$	—	—	—	∞	—	G_2 block
<i>mik1Δwee1^{ts}cdc25Δ</i>	$V_{Mik1} = V_{Mik} = 0, V_{Wee} = 0.08, V_{25} = V_{25} = 0$	No balanced growth, S and M overlap					<i>cut</i> phenotype
<i>wee1^{ts}cdc25^{ts}</i>	$V_{Wee} = 0.08, V_{25} = 0.05, V_{25} = 0.00025$	0.80	37	17	69	27	
<i>wee1Δcdc25Δ</i>	$V_{Wee} = V_{Wee} = 0, V_{25} = V_{25} = 0$	0.76	40	18	65	27	
<i>rum1Δ</i>	$k_5 = 0$	0.99	31	17	84	18	
<i>rum1Δwee1^{ts}</i>	$k_5 = 0, V_{Wee} = 0.08$	0.41	24	18	77	31	Not viable [§]
<i>ste9Δ</i> or <i>cdc13dbΔ</i>	$V_2 = V_{2c} = 0$	0.84	12	18	102	18	
<i>ste9Δwee1^{ts}</i>	$V_2 = V_{2c} = 0, V_{Wee} = 0.08$	0.30	1	18	98	33	Not viable [§]
<i>ste9Δrum1Δ</i>	$V_2 = V_{2c} = 0, k_5 = 0$	0.82	12	18	102	18	
<i>ste9Δrum1Δwee1^{ts}</i>	$V_2 = V_{2c} = 0, k_5 = 0, V_{Wee} = 0.08$	0.28	0	19	98	33	Not viable [§]

*Parameter changes relative to the WT set (Table 1) are indicated.

[†]The duration of the appropriate cell cycle phase is given. M phase is initiated when MPF crosses 0.5 from below and it finishes 5 min after MPF_a/PP drops below 0.5. The rules for the onset and completion of S phase are described in Table 1.

[‡]As a consequence of the quantized cycles, these cells do not behave uniformly. Mean values of cells having the short cycle and the longer cycle, respectively, are separated by/. In the long cycle, during the 107-min G_2 phase, there is a short period with high MPF, probably indicating an early M-like state (see text).

[§]Cells significantly smaller than a *wee1⁻* mutant are considered too small to be viable.

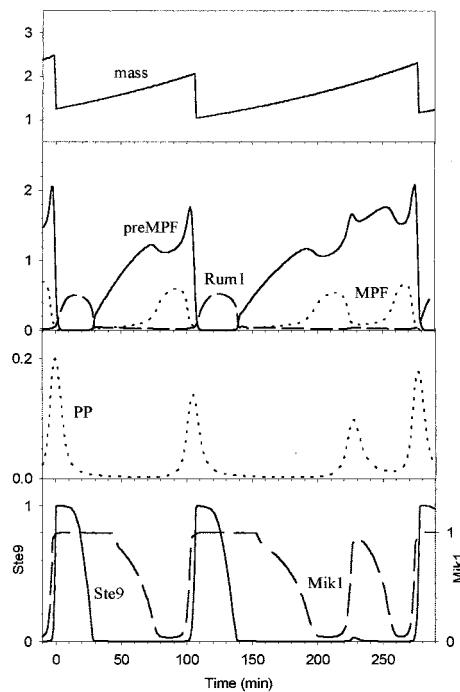


Fig. 4. Numerical simulation of *wee1^{ts} cdc25Δ* double mutant cells.

well as Mik1, thus resetting the cell to G₁ phase. Possibly the transient activation of Cdc13/Cdc2 halfway through the long cycle initiates some early events of mitosis, because cell elongation slows down in such cells (32), which normally indicates that the cell has entered mitosis (33). It is also noteworthy that periodic chromosome condensation and decondensation was recently observed in an *Aspergillus nidulans* mutant, corresponding to reversible mitotic entry and exit (34).

If relative cell mass at birth is larger than about 1.16 (mass at birth is 1.0 for WT cells), then the first activation of MPF will drive the cell through proper mitosis and reset its progeny to G₁ phase. Because the cell has a short CT, less than the mass doubling time, its progeny will be smaller at birth than their mother was at birth. If the daughter cells are born smaller than 1.16, they will start a long cell cycle and give rise to large granddaughters. Hence, both birth size and CT will be highly variable in cultures of *wee1^{ts} cdc25Δ* cells.

It is worth noting that cycle-time quantization only occurs in the total absence of Cdc25 ($V_{25}^{\prime} = V_{25} = 0$); *wee1^{ts} cdc25^{ts}* double mutant cells show a semi-*wee* phenotype with a 150-min generation time (Table 2), in accordance with experiments (35, 36). There is no experimental data on the behavior of *wee1Δ cdc25Δ* cells, but the model predicts them to have a semi-*wee* phenotype (Table 2), suggesting that residual Wee1 activity in *wee1⁻ cdc25Δ* is required for cycle-time quantization.

In this deterministic model, the CT of individual *wee1^{ts} cdc25Δ* cells is absolutely determined by cell mass at birth: large cells (relative mass > 1.16) show short cycles, whereas small cells (mass < 1.16) show long cycles. In experiments, no such size threshold is observed: cells of the same mass may have short or long cycles (although very large cells have always the shortest CT) (12). Also, with the parameter values used to simulate Fig. 4, there are no cycles with two resettings to G₂ phase, which would account for the 230-min cycles observed experimentally. However, we have found that these quantized cycles are very sensitive to low, constant activity of Pyp3. Slightly smaller V_{Pyp} values often result in very long cycles (CT > 220 min) with two resettings to G₂ phase. For these reasons, we have introduced some stochastic “noise” into our

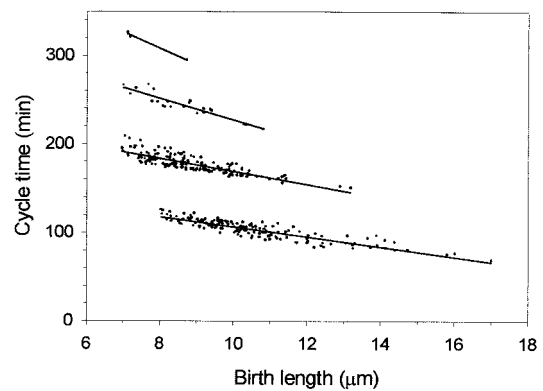


Fig. 5. CT vs. BL relationship for simulated *wee1^{ts} cdc25Δ* cells. This graph should be compared with the experimental data in figure 6A from ref. 12.

simulations, to give a better account of quantized cycles. It is worth mentioning that *wee1^{ts} cdc25Δ* cells become nonviable if either *pyp3* or *mik1* are deleted (21); our simulations are consistent with the phenotypes of the appropriate triple mutants.

A Stochastic Model

Probably the activities of all proteins involved in our model, as well as the rate constants of the biochemical reactions, are stochastic variables, but it is unnecessary to take all possible stochastic variability into account. Because Pyp3 plays an important role in regulating these quantized cycles, we treat its rate parameter (V_{Pyp}) alone as a stochastic variable. From cycle to cycle, we assign to V_{Pyp} a random number chosen from a normal distribution with mean 0.07 min^{-1} and standard deviation 0.02 min^{-1} .

With this stochastic model, we simulated more than 300 cells and plotted CT as a function of birth mass (Fig. 5). To make this figure directly comparable with experimental data in figure 6A from ref. 12, we have assumed that 1 unit of mass corresponds to 8.2- μm cell length. Our model simulates the experimental data very well. In particular, birth length (BL) no longer determines to which group a cell belongs, except for very large cells (BL > 13 μm), which have the minimum CT because they never reset to G₂, as observed (12, 32). Our simulations predict a small population of cells with CT > 300 min (three resettings to G₂). Such cells have not been observed, perhaps because the durations of the films were not long enough to find them.

Robustness of the Model

Division size of fission yeast depends sensitively on the gene dosages of *wee1* and *cdc25* (18, 30). Fission yeast tolerates reduced and excess levels of these regulators over wide ranges. To test whether our model is consistent with such robust behavior, we varied the parameters representing turnover numbers of Wee1 and Cdc25 over wide ranges (with all other parameters set to the values in Table 1). Fig. 6 exhibits curves of constant BL on the plane of variable Wee1 and Cdc25 activities. These iso-BL curves run more or less diagonally, with decreasing mass values from left to the right. As a consequence, moving to the right (by increasing Cdc25 activity) or moving down (by reducing Wee1 activity) results in a decrease in BL, as observed (18, 30). Cells show balanced growth and division over wide ranges of Wee1 and Cdc25 activities, demonstrating the robustness of the model. In this broad region of parameter space, CT is always the same as mass-doubling time; only cell masses at birth and division are changing as functions of Wee1 and Cdc25 activities. We have divided the area of balanced growth and division somewhat arbitrarily into two regions: cells smaller than

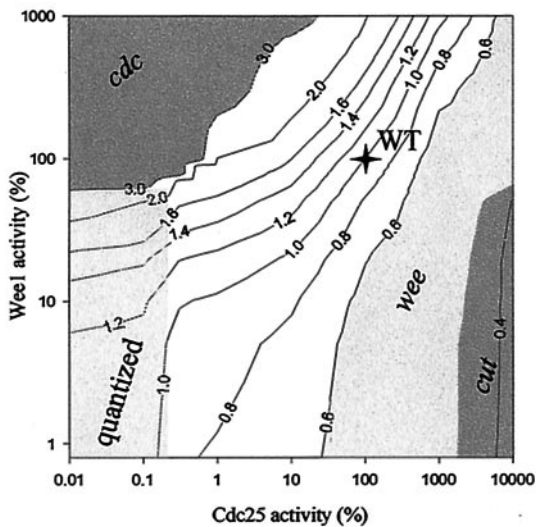


Fig. 6. Effects of Wee1 and Cdc25 activities on BL and phenotype of fission yeast. Curves represent cells of constant BL (BL = 1.0 for WT cells). The shaded regions represent different cells phenotypes. Both enzyme activities are expressed as percentage of WT. For Wee1 (ordinate), we varied only the large turnover number (V_{Wee}), leaving the small one (V_{Wee}) unchanged. For Cdc25, we varied both (V_{25} and V_{25}), keeping their ratio the same as in WT.

60% of WT are considered *wee*, whereas cells in the range $0.6 < BL < 3$ are more or less normal.

Outside the area of balanced growth and division, in the upper left corner of Fig. 6 ($BL > 3$), cell mass at division increases abruptly, and these cells can be treated as *cdc*. In the lower right corner, cells show mitotic catastrophe because they activate MPF prematurely and divide before they can finish S phase. This is fully consistent with the *cut* phenotype found in *wee1⁻cdc25^{op}* mutants (30). By contrast, cells in the lower left corner (with low Wee1 and Cdc25 activities) have more than one CT (quantized cycles). Because the area in parameter space of quantized cycles is extensive, the phenomenon is a robust characteristic of our model.

Discussion

The idea of quantized cycles has a long history in cell cycle research (37, 38), but has not been widely accepted for two major reasons: the experimental evidence was not convincing, and the clock driving these quantized cycles was obscure. We think that the

situation has changed on both fronts. First, clear evidence for quantized cycles has been observed in *wee1⁻cdc25 Δ* fission yeast cells (12) and in *Xenopus* oocytes (39). Second, in this paper we propose that quantized cycles in *wee1⁻cdc25 Δ* fission yeast cells are simply a consequence of free-running oscillations of an underlying cell cycle engine rather than manifestations of an independent ultradian clock as proposed by Kippert and Hunt (40). Our model is similar to the idea proposed by Shymko *et al.* (37).

The cell division cycle clearly has an underlying molecular clock that drives major cell cycle events, like DNA replication and mitosis. However the free-running clock is only apparent in cells with an abnormally high protein-to-DNA ratio; for example, early embryos or *cdc^{ts}* yeast cells that have been held temporarily at the restrictive temperature. By contrast, in normal vegetative or somatic cells, the operation of the cell cycle clock is controlled by surveillance mechanisms (checking the replication state of DNA and cell size) that stop the clock at specific cell cycle checkpoints. These checkpoints are stable steady states of the regulatory system. A checkpoint is lifted, and the cell progresses to the next stage of the cycle, only if certain conditions are satisfied. These stable checkpoints are consequences of antagonistic relationships between cell cycle regulators. For example, in WT fission yeast, the positive feedback loops in Cdc2 Tyr-15 phosphorylation create two stable states with low and high Cdk activity, corresponding to interphase and mitosis. As a consequence of positive feedback, the transitions between these two states are all-or-none. The mitotic state is destabilized at the end of mitosis by a slow negative feedback loop, which up-regulates the enemies of MPF. If the positive feedback loops are weak, as in the *wee1⁻cdc25 Δ* mutant, then the mitotic control network starts to oscillate, as a consequence of an underlying clock mechanism based on the negative feedback loop (41). Although spontaneous oscillations in the cell cycle engine are reminiscent of early embryos, these double mutant cells do not always divide at the period of the limit cycle oscillator, because cell mass exerts a gating effect. If cell mass is too small, then mitosis cannot be completed the first time it is initiated. Instead, the cell reverts to G_2 , grows larger, and tries again. As a consequence, age at division is clearly quantized in these double mutant cells.

We dedicate this paper to Prof. Murdoch Mitchison, who introduced us to cell cycle research. We thank Dr. Sergio Moreno for helpful discussions and communicating unpublished results. Our research was supported by the Howard Hughes Medical Institute (75195-542501), the Hungarian Scientific Research Fund (OTKA F-022176 and T-032015), and the National Science Foundation (DBI-9724085). A.S. is grateful to the Hungarian Higher Education and Research Foundation for a Zoltan Magyary Postdoctoral Fellowship.

- Nurse, P. (1994) *Cell* **79**, 547–550.
- Fisher, D. L. & Nurse, P. (1996) *EMBO J.* **15**, 850–860.
- Stern, B. & Nurse, P. (1996) *Trends Genet.* **12**, 345–350.
- Novak, B., Csikasz-Nagy, A., Gyorffy, B., Chen, K. & Tyson, J. J. (1998) *Biophys. Chem.* **72**, 185–200.
- Correa-Bordes, J. & Nurse, P. (1995) *Cell* **83**, 1001–1009.
- Benito, J., Martin-Castellanos, C. & Moreno, S. (1998) *EMBO J.* **17**, 482–497.
- Tourret, J. & McKeon, F. (1996) *Prog. Cell Cycle Res.* **2**, 91–97.
- Aligue, R., Wu, L. & Russell, P. (1997) *J. Biol. Chem.* **272**, 13320–13325.
- Kovelman, R. & Russell, P. (1996) *Mol. Cell. Biol.* **16**, 86–93.
- Visintin, R., Craig, K., Hwang, E. S., Prinz, S., Tyers, M. & Amon, A. (1998) *Mol. Cell* **2**, 709–718.
- Jaspersen, S., Charles, J. & Morgan, D. (1999) *Curr. Biol.* **9**, 227–236.
- Sveiczzer, A., Novak, B. & Mitchison, J. M. (1996) *J. Cell Sci.* **109**, 2947–2957.
- Novak, B., Csikasz-Nagy, A., Gyorffy, B., Nasmyth, K. & Tyson, J. J. (1998) *Philos. Trans. R. Soc. London B* **353**, 2063–2076.
- Novak, B., Toth, A., Csikasz-Nagy, A., Gyorffy, B., Tyson, J. J. & Nasmyth, K. (1999) *J. Theor. Biol.* **199**, 223–233.
- Yamaguchi, S., Murakami, H. & Okayama, H. (1997) *Mol. Biol. Cell* **8**, 2475–2486.
- Kitamura, K., Maekawa, H. & Shimoda, C. (1998) *Mol. Biol. Cell* **9**, 1065–1080.
- Labib, K. & Moreno, S. (1996) *Trends Cell Biol.* **6**, 62–66.
- Russell, P. & Nurse, P. (1987) *Cell* **49**, 559–567.
- Lundgren, K., Walworth, N., Booher, R., Dembski, M., Kirschner, M. & Beach, D. (1991) *Cell* **64**, 1111–1122.
- Murray, A. & Hunt, T. (1993) *The Cell Cycle: An Introduction* (Freeman, New York).
- Millar, J. B. A., Lanaers, G. & Russell, P. (1992) *EMBO J.* **11**, 4933–4941.
- Fisher, D. & Nurse, P. (1995) *Semin. Cell Biol.* **6**, 73–78.
- Martin-Castellanos, C., Labib, K. & Moreno, S. (1996) *EMBO J.* **15**, 839–849.
- Matsumoto, T. (1997) *Mol. Cell. Biol.* **17**, 742–750.
- Goldbeter, A. & Koshland, D. E., Jr. (1981) *Proc. Natl. Acad. Sci. USA* **78**, 6840–6844.
- Creanor, J. & Mitchison, J. M. (1994) *J. Cell Sci.* **107**, 1197–1204.
- Moreno, S. & Nurse, P. (1994) *Nature (London)* **367**, 236–242.
- Schwab, M., Lutum, A. S. & Seufert, W. (1997) *Cell* **90**, 683–693.
- Yamano, H., Gannon, J. & Hunt, T. (1996) *EMBO J.* **15**, 5268–5279.
- Russell, P. & Nurse, P. (1986) *Cell* **45**, 145–153.
- Enoch, T., Gould, K. L. & Nurse, P. (1991) *Cold Spring Harbor Symp. Quant. Biol.* **56**, 409–416.
- Sveiczzer, A., Novak, B. & Mitchison, J. M. (1999) *J. Cell Sci.* **112**, 1085–1092.
- Mitchison, J. M. & Nurse, P. (1985) *J. Cell Sci.* **75**, 357–376.
- Ye, X. S., Fincher, R. R., Tang, A., Osmani, A. H. & Osmani, S. A. (1998) *Mol. Biol. Cell* **9**, 3019–3030.
- Fantes, P. (1979) *Nature (London)* **279**, 428–430.
- Grallert, A., Grallert, B., Ribar, B. & Sipiczki, M. (1998) *J. Bacteriol.* **180**, 892–900.
- Shymko, R. M., Klevecz, R. R. & Kaufmann, S. A. (1984) in *Cell Cycle Clocks*, ed. Edmunds, L. N., Jr. (Dekker, New York), pp. 273–293.
- Lloyd, D., Poole, R. K. & Edwards, S. W. (1982) *The Cell Division Cycle: Temporal Organization and Control of Cellular Growth and Reproduction* (Academic, London).
- Masui, Y. & Wang, P. (1998) *Biol. Cell* **90**, 537–548.
- Kippert, F. & Hunt, P. (2000) *BioEssays* **22**, 16–22.
- Goldbeter, A. (1991) *Proc. Natl. Acad. Sci. USA* **88**, 9107–9111.